# SYNTHESIS AND CHARACTERIZATION OF NICKEL, COBALT AND Ni-DOPED COBALT HYDROXIDES

A THESIS SUBMITTED IN PARTIAL FULFILLMENT

OF THE REQUIREMENTS FOR THE DEGREE OF

**Bachelor of Technology**

**in**

**Ceramic Engineering**

By

**MADHUR KUMAR LENKA**

Under the Guidance of

**Prof. Bibhuti B. Nayak**


Department of Ceramic Engineering
National Institute of Technology
Rourkela 769008 Odisha

**Department of Ceramic Engineering**
**National Institute of Technology, Rourkela**
**Rourkela – 769 008, Odisha, India**

# CERTIFICATE

This is to certify that the thesis entitled "SYNTHESIS AND CHARACTERIZATION NICKEL, COBALT and Ni DOPED COBALT HYDROXIDES", submitted by Mr. Madhur Kumar Lenka bearing Roll number**:** 111CR0100 in partial fulfilment of the requirements for the award of Bachelor of Technology in Ceramic Engineering at National Institute of Technology, Rourkela is an authentic work carried out by him under my supervision and guidance.

To the best of my knowledge, the matter embodied in the thesis has not been submitted to any other university/institute for the award of any Degree or Diploma.

PLACE: ROURKELA
Date: -

Prof. Bibhuti Bhusan Nayak
Dept. of Ceramic Engineering
National Institute of Technology
Rourkela – 769008

# ACKNOWLEDGEMENTS

I wish to express my deep sense of gratitude and indebtedness to Prof. Bibhuti B. Nayak, Department of Ceramic Engineering, National Institute of Technology Rourkela for introducing the present topic and for his inspiring guidance and valuable suggestion throughout this project work. I am also thankful to all faculty members as well as staff members of Department of Ceramic Engineering, NIT Rourkela. I am also thankful to Mr. Nadiya Bihary Nayak, Sourav Mondal and other research scholars in Department of Ceramic Engineering for providing all joyful environment in the lab and helping me out in different ways.

Madhur Kumar Lenka

# CONTENTS

# LIST OF FIGURES

# ABSTRACT

In the current research work nickel hydroxide, cobalt hydroxide and Ni-doped cobalt hydroxide powders were synthesized through the precipitation method by using 0.5 molar sodium hydroxide solution, 1 molar nickel chloride hexahydrate, cobalt chloride hexahydrate solution respectively along with hydrazine hydrate solution. Morphology of as-synthesised powders indicated spherical structure of nickel hydroxide and polyhedral structure of cobalt hydroxide. The surface morphology of the doped sample was similar to cobalt hydroxide because of higher amount of cobalt present in the doped sample. The DSC-TG curve shows that there is maximum percentage of mass loss at around $300^0$C which is due to conversion of nickel hydroxide into nickel oxide and for cobalt hydroxide and the doped sample the weight loss happened around $170^0$C.The photoluminescence test of the hydroxide and oxide samples are carried out. The result showed all the hydroxides have photoluminescence property in the violet-blue region. But among the calcined powders (300 °C), calcined nickel hydroxides and Ni-doped cobalt hydroxide showed the same violet-blue luminescence.



Key words: nickel hydroxide, cobalt hydroxide, Ni-doped cobalt hydroxide, photoluminescence

## INTRODUCTION:

As one of the quickly growing areas, nanomaterials have fascinated notable attentions in contemporary years because of typically possessing enhanced magnetic, optical, thermal and catalytic properties compared to their individual component materials. Nickel/cobalt based nanomaterials in the form of hydroxides or oxides are becoming a research focus owing to their extensive applications in super capacitors as electrode materials. Among them due to their cost effective and environmentally benign properties cobalt-nickel double hydroxides may have widespread applications in super capacitors, pseudo capacitors, electro catalysis, photocatalysis and rechargeable batteries.

Nickel hydroxide ($Ni(OH)_2$) has enticed increasing interests because of its applications in alkaline rechargeable batteries (such as Ni/MH, Ni/Zn, Ni/Cd, and Ni/Fe), which are most extensively used in numerous applications ranging from power tools to portable electronics and electric vehicles. Nickel (II) hydroxide has two well-characterized pseudopolymorphs, its α and β forms [1]. The α structure consists of $Ni(OH)_2$ layers with intercalated anions or water molecules occupying the space between layers. The β form is a hexagonal closest-packed structure of $Ni^{2+}$ and $OH^-$ ions, without other intercalated ions. Among these two phases, due to its intrinsic lamellar structure single-crystalline $\beta$-$Ni(OH)_2$ nanosheets have been demonstrated and widely used because of its high stacking density and stability in alkaline condition in contrast with $\alpha$-$Ni(OH)_2$. Due to more crystalline defects and smaller crystalline size $Ni(OH)_2$ shows a higher chemical proton diffusion coefficient, and this will diminish the concentration polarization of protons throughout charge/discharge cycle, leading to a better charge/discharge cycling behaviour. Literatures have stated that the activity of $Ni(OH)_2$ electrode could be substantially enhanced when nanosized $Ni(OH)_2$ is added into microsized $Ni(OH)_2$; especially, nanosized $Ni(OH)_2$ [2] with mesoporous structures can improve the electrochemical performance greatly. Moreover, NiO is a significant p-type semiconductor with a direct band gap of 3.5 eV and often used as catalyst, electrochemical capacitor, fuel cell electrode, gas sensor and so forth. NiO can be obtained by calcinating the corresponding $Ni(OH)_2$ in air, and the shape of $Ni(OH)_2$ particles could be retained.

Cobalt hydroxide and cobalt oxides are especially fascinating due to their exceptional physical and chemical properties, which make them favourable materials broadly applied in rechargeable Li-ion batteries, gas sensing catalysis, ionic exchangers and magnetic

materials and others. The oxides of cobalt are also a vital precursor in sol-gel technique for preparing high-purity and high-strength monolithic cobalt oxide ceramics for usage as substrates for electronic circuits, abrasive grains, high-temperature refractory materials, fibres, and thin films. Cobalt oxide ($Co_3O_4$) is an important magnetic p-type semiconductor with an indirect band gap of 1.5 eV. $Co(OH)_2$ itself is well known as an additive of alkaline secondary batteries[3]; it is also an important starting materials of heterogeneous catalysts and precursor for CoO(OH) and $Co_3O_4$ materials.

Lately, composite materials, such as composites of metal oxides ($Co_3O_4$-$MnO_2$, $MnO_2$–NiO etc.) and binary metal oxide/hydroxides [4] ($Ni(OH)_2$–$MnO_2$, $Co_3O_4$–$Ni(OH)_2$, etc.), have been the focus in the field of pseudo capacitors. In these hybrid structures, both individual constituents are good pseudo capacitive materials, contributing to the electrochemical charge storage. Moreover, the hybrid structure can combine the qualities of both components, which may bring a strong synergistic effect on the excellent electrochemical performances of the electrodes.

## LITERATURE REVIEW:

Yumei Ren *et al.* [5] synthesized β-$Ni(OH)_2$ nanoplates by a hydrothermal process with sodium hydroxide as precipitator and nickel nitrate as nickel source. They found with molar ratio of $Ni^{2+}$:$OH^-$ 1:1, reaction time 4h, reaction temperature 180℃ , pH value of reaction mixture 10, β-$Ni(OH)_2$ nanoplates can be synthesized with regular hexagonal morphology, good dispersion, narrow particle size distribution range and large width-to-thickness ratio. Through electrochemical performance tests, β-$Ni(OH)_2$ showed a structure-dependence in their specific charge capacitances. Quansheng Song *et al.* [6] studied the structural characteristics of nickel hydroxide synthesized by a chemical precipitation route under different pH values. The structural characteristics of the synthesized β-$Ni(OH)_2$, such as degree of crystallinity, crystalline lattice disorders, crystallite size and crystal growth orientation were strongly related to the pH values of the chemical precipitation reaction. The amounts of sulphate, carbonate and water species adsorbed in crystals, and the thermal stability of the β-$Ni(OH)_2$ also depended on the pH. Under relatively high pH values, the synthesized nickel hydroxide materials possessed a reduced crystallite size and lower thermal stability, more crystalline defects and a higher Ni composition. Wei Xing *et al.* [7] synthesized a novel mesoporous nickel hydroxide with very high surface area with an anionic sulfate template. The BET surface area of NiO

calcined at 250 °C is found to be 477.7$m^2$ $g^{-1}$. From the results of Nitrogen adsorption and XRD analysis they found that $Ni(OH)_2$ and calcined NiO have good mesoporous structures. Cyclic voltammetry indicated a good capacitive behaviour for mesoporous NiO samples and this C-V behaviour improved with increase in calcination temperature. Galvanostatic discharge indicates that the capacitance of NiO is determined by two factors, namely, surface area and surface reactivity. Taking these two factors into consideration, calcination at 250 °C gives the highest capacitance, i.e., 124 F $g^{-1}$. On the other hand, NiO calcined at 300 °C possesses the highest surface redox reactivity. Zhang YongQi *et al.* [8] prepared a porous $Co(OH)_2$ film, consisting of randomly porous nanoflakes with thicknesses of 20 nm and directly grown on nickel foam by a facile hydrothermal method. The porous $Co(OH)_2$ film exhibited a high discharge capacitance of 935 F $g^{-1}$ at 2 A $g^{-1}$ and excellent rate capability. They found out excellent electrochemical capacitive performance is mainly due to the high porosity and large surface area of the porous architecture. DongEn Zhang *et al.* [9] synthesized $Co_3O_4$ multilayered structures were by a facile poly (ethylene glycol 20000) (PEG-20000) assisted hydrothermal technique in combination with calcination method. Experimental results obtained from the different growth stages demonstrated that the as-prepared precursor exhibited an interesting time-dependent evolution of building blocks, from urchin to multilayer. The possible formation mechanism for the hierarchical structures with various architectures was presented on account of the self-assembled growth induced by Ostwald ripening. The photocatalytic activity of the products was also examined by measuring the photo decolourisation of methyl violet solution with ultraviolet radiation. The result showed that the products have a good photocatalytic activity. Guoping Wang *et al.* [10] synthesized a composite $Ni_{0.37}Co_{0.63}(OH)_2$ material via a chemical precipitation method with the purpose to develop electrode materials for super capacitors. They characterized the material with Instrumental methods such as XRD, EDX, and SEM. The results showed that $Ni_{0.37}Co_{0.63}(OH)_2$ possessed an amorphous structure, which provides a higher specific capacitance (1840 F $g^{-1}$). The electrochemical measurements showed that $Ni_{0.37}Co_{0.63}(OH)_2$ could give a two-electron redox process accompanied by two $OH^-$ ions. They recorded Cyclic voltammogram curves of $Ni_{0.37}Co_{0.63}(OH)_2$ and used to measure specific capacitances at different potential scan rates and concluded if $Ni_{0.37}Co_{0.63}(OH)_2$ was used to construct a supercapacitor, the charging/discharging process will then be limited to low potential scan rates. Jinxiu Li *et al.* [11] prepared a Doughnut-like nanostructured $Ni(OH)_2$–$Co(OH)_2$ composite by combining hydrothermal and chemical deposition routes. They investigated

electrochemical performances of the composites as pseudocapacitor materials through galvanostatic charge–discharge and cyclic voltammetry tests. The $Ni(OH)_2$–$Co(OH)_2$ composites delivered a specific capacitance of 2193 F $g^{-1}$ at 2 A $g^{-1}$ and 1398 F $g^{-1}$ at 20 A $g^{-1}$, much higher than those of pristine $Ni(OH)_2$. They concluded enhancement of the overall electrochemical performances is due to the synergetic contribution from nanostructured $Ni(OH)_2$ and electrically conductive CoOOH forming in the charge process. In the following charge–discharge process, CoOOH serves as both the conductive network and the active material, which has a big advantage over those in pseudocapacitive carbon-based conductive materials in improving both the energy density and power density of pseudocapacitor electrodes. Wenzhong Wang *et al.* [12] developed a two step strategy for the preparation of pure cubic phase $Co_3O_4$ porous nano plates. Firstly they prepared a α-$Co(OH)_2$ nanoplates by a facile surfactant free low temperature solution phase method. Then $Co_3O_4$ nanoplates were obtained by thermal decomposition of the as synthesized α-$Co(OH)_2$ nanoplates at 400 °C for 2 h in air.

## EXPERIMENTAL WORK

### 3.1 Synthesis of Nickel Hydroxide, Cobalt Hydroxide and Ni-doped Cobalt Hydroxide

For the preparation of nickel hydroxide, nickel chloride hexahydrate ($NiCl_2.6H_2O$), hydrazine hydrate ($N_2H_5OH$) and NaOH was taken as starting materials. Hydrazine hydrate and NaOH was added drop by drop through a burette to a beaker containing Ni-salt. From the above solution precipitate of nickel hydroxide is formed at higher pH. The obtained powders were washed several times with hot DI water. Then the precipitate was collected by filtering the solution with Whatmann filter paper. The filtrate was dried for 24 hours at $60^0$C. The dried mass was grinded properly using agate mortar to get fine powder of nickel hydroxide.

For the preparation of cobalt hydroxide and Ni-doped cobalt hydroxide the exact same process was followed. But instead of molar solution of nickel hexahydrate molar solution of cobalt hexahydrate is used for preparing cobalt hydroxide. For preparation of Ni-doped cobalt hydroxide molar solution of cobalt hexahydrate and nickel hexahydrate was taken in ratio of 9:1 in the same amount.

The three obtained powders were calcined at $300^0$C and $500^0$C in pit furnace with 1 hour soaking time.

## 3.2 General Characterization:

### 3.2.1 Thermal Analysis:

Thermal decomposition of $Ni(OH)_2$ powder to NiO, $Co(OH)_2$ to CoO and Co-$Ni(OH)_2$ powder was studied using thermogravimetric and differential scanning calorimetry DSC/TG by heating the sample at 10°C/min in Argon atmosphere in a thermal analyser (Model Netzsch, STA 449C). Alpha alumina was used as reference material.

### 3.3.3 X-ray Diffraction:

Phase analysis was studied using the X-ray diffraction (Rigaku, Japan) at room temperature with filtered 0.154056 nm Cu-Kα radiation. Samples were scanned in a continuous mode from 200-800 at a scanning rate of 200/min.

### 3.3.4 Microstructural analysis:

Microstructural features were studied using Felid Emission Scanning Electron Microscope (NOVA, NanoSEM). One pinch of the well-grinded sample powder was deposited on to the carbon tape pasted on the brass plate. This brass plate was coated for 5 minutes and then used for microscopy.

### 3.3.5 Photoluminescence

Photoluminescence properties of the prepared samples were studied by exposing the sample to different emissions and acquiring the excitation spectra of the samples. All the samples were excited at 220 nm to get the emission spectra.

# RESULTS AND DISCUSSION

## 4.1 Thermal Analysis (DSC-TG):

Figure 1 shows the DSC-TG curves of as synthesized nickel hydroxide powder. Two endothermic peaks were observed in the DSC curve, in which the first endothermic peak is around $100^0$C because of the removal of absorbed water molecules and the second peak at around $300^0$C corresponds to the decomposition of nickel hydroxide into nickel oxide. The weight loss in TG curve also aligns with the endothermic peaks in which a mass loss of about 5% occurs before $200^0$C due to removal of water and about 15% mass loss occurs at around $300^0$C due to conversion of nickel hydroxide into nickel oxide.

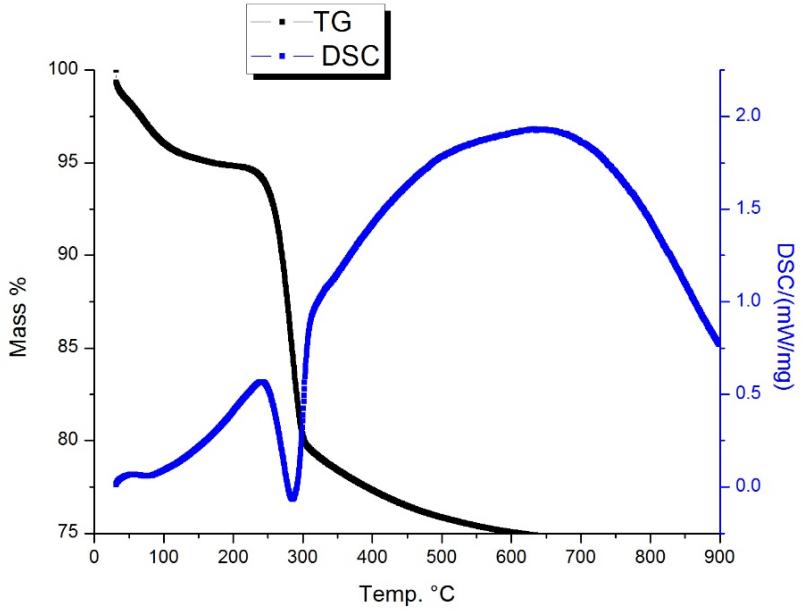


*Figure 1: DSC-TG curve of as synthesized $Ni(OH)_2$ powder*

Fig 2 & 3 show the DSC-TG curves for $Co(OH)_2$ and Co-$Ni(OH)_2$ respectively. These two samples have relatively similar graphs. In case of $Co(OH)_2$, an exothermic peak was observed at around $175^0$C which indicates the conversion of cobalt hydroxide into cobalt oxide. The TG curve supports it with a 5% weight loss. In case of the Co-$Ni(OH)_2$ sample, the exothermic peak shifts to $190^0$C and the TG curve shows a weight loss of around 7% due to the conversion of the hydroxides into oxides.

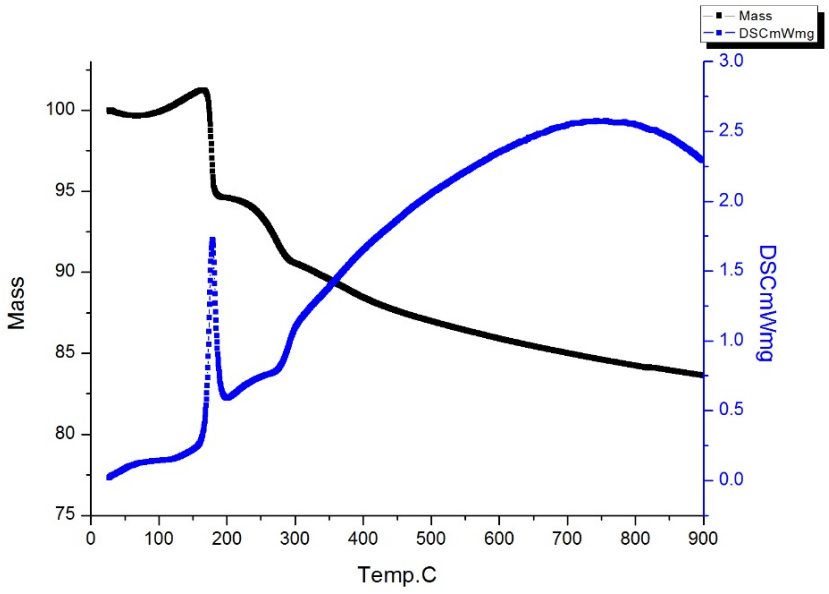


*Figure 2: DSC-TG of as synthesized $Co(OH)_2$ powder*

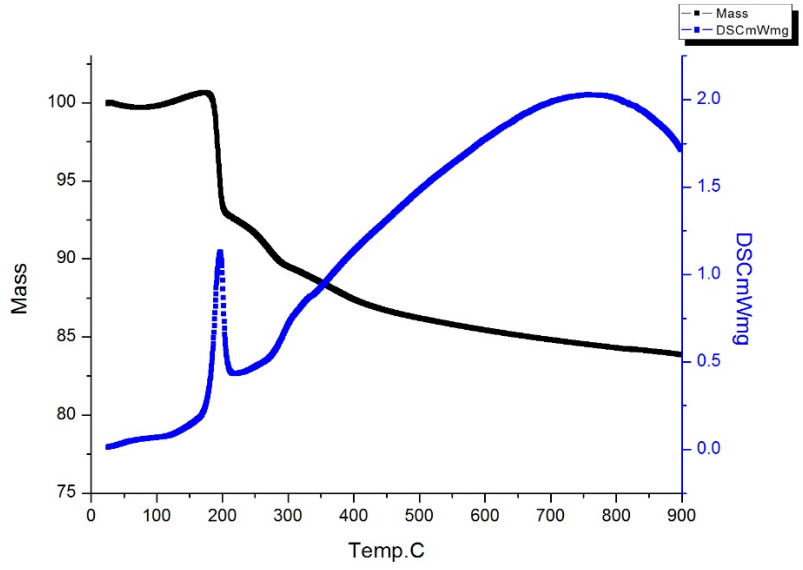


*Figure 3: DSC-TG curve of as synthesized Co-$Ni(OH)_2$ powder*

## 4.2 Structural Analysis (XRD):

The results of XRD analysis of as-synthesized and calcined $Ni(OH)_2$, $Co(OH)_2$ and Co-$Ni(OH)_2$ samples are shown in Figure 4 to 12. Figure 4, 5 and 6 show the XRD patterns of as synthesized $Ni(OH)_2$, calcined $Ni(OH)_2$ at $300^0$C and $500^0$C respectively. All the peaks in case of as-synthesized $Ni(OH)_2$ match with ICSD-98-002-8101. The crystal system is hexagonal and '*d*' spacing is 2.33(9) Å.

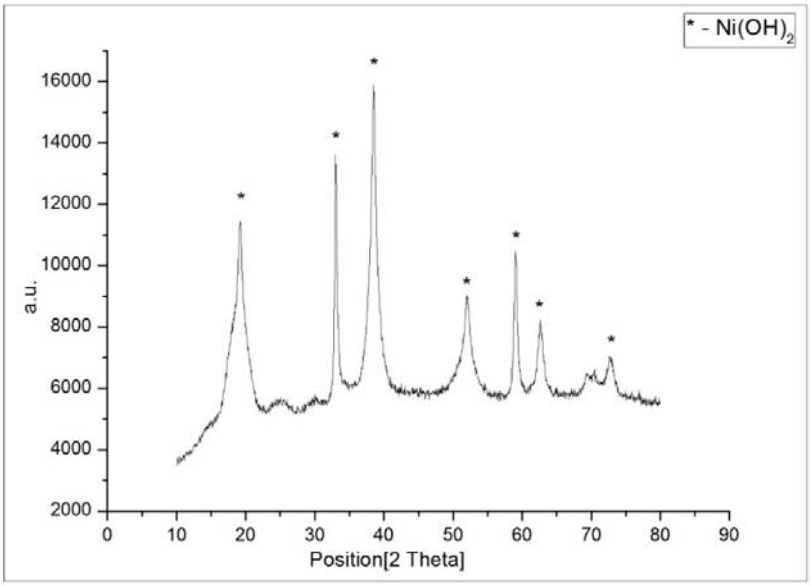


*Figure 4: XRD patterns of as synthesized $Ni(OH)_2$ powder*

All peaks in case of $Ni(OH)_2$ calcined at $300^0$C match with ICSD-98-016-6122. The crystal structure is hexagonal and '*d*' spacing is 2.09(4) Å. At this temperature, the $Ni(OH)_2$ has converted to NiO.

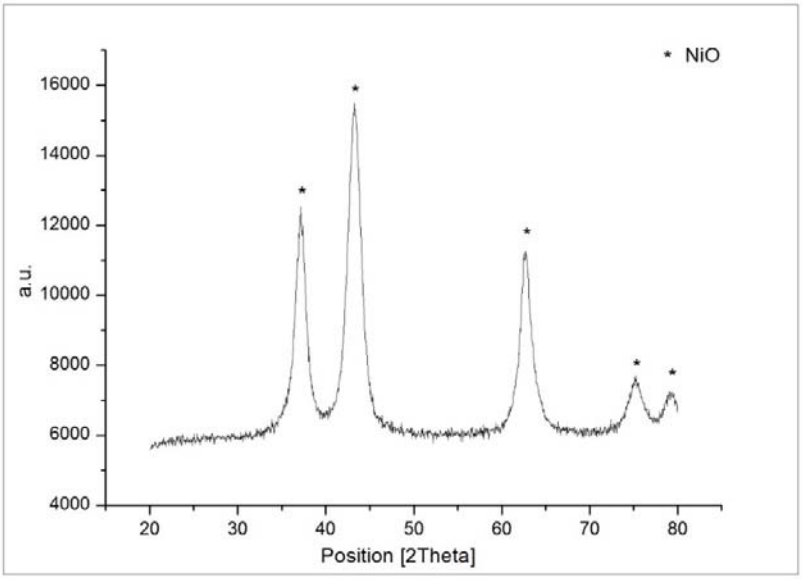


*Figure 5: XRD patterns of $Ni(OH)_2$ calcined at $300^0$C*

When calcined at $500^0$C, all the peaks match with ICSD-98-069-6096. But the crystal structure in this case has been transformed to cubic and the '*d*' spacing has become 2.09 Å

i.e. decreased marginally. Also, an enhanced crystallinity can be observed with the increasing calcination temperature.

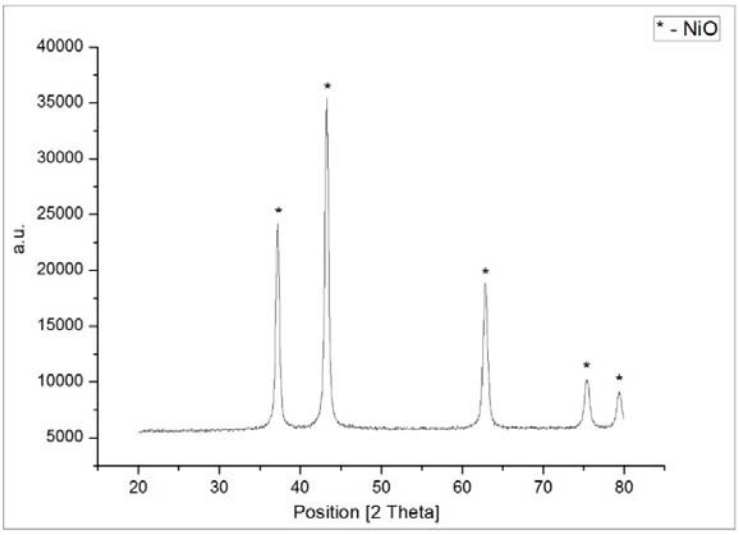


*Figure 6: XRD patterns of $Ni(OH)_2$ calcined at $500^0C$*

Figure 7, 8 and 9 show XRD patterns of as-synthesized $Co(OH)_2$ , calcined $Co(OH)_2$ at $300^0C$ and $500^0C$, respectively. All the peaks in case of as synthesized $Co(OH)_2$ match with ICSD-98-002-6763. The crystal structure is cubic.

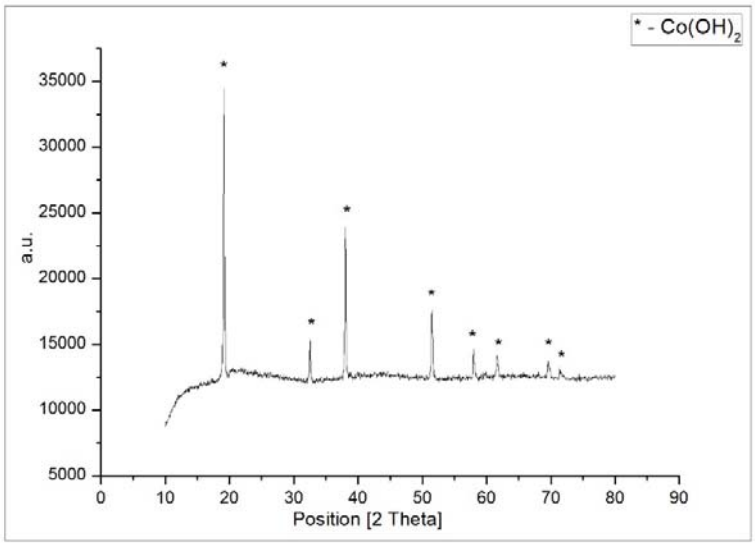


*Figure 7: XRD patterns of as synthesized $Co(OH)_2$*

When calcined at 300°C, all peaks match with ICSD-98-006-9365. The compound found is $Co_3O_4$. The crystal structure is cubic with *'d'* spacing 2.43(6) Å.

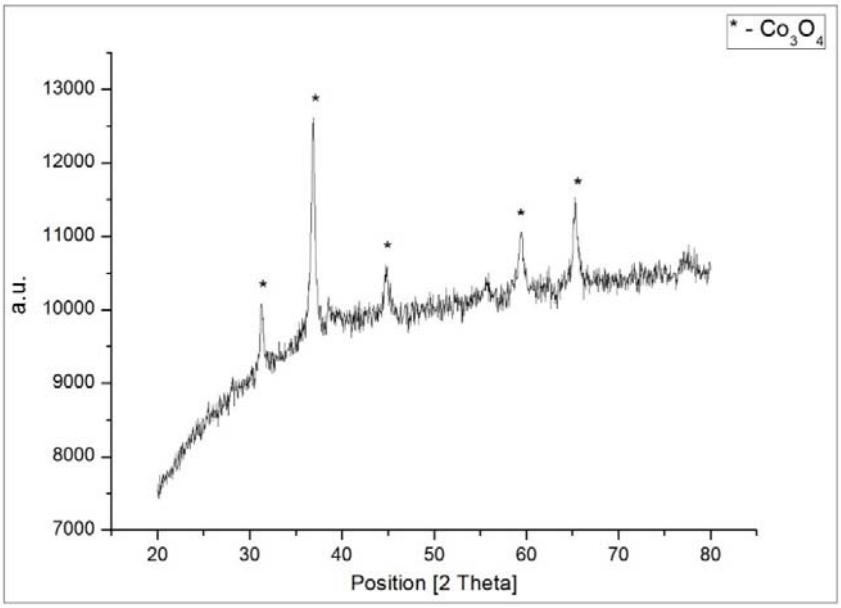


*Figure 8: XRD patterns of $Co(OH)_2$ calcined at $300^0C$*

When calcined at 500 °C, all the peaks match with ICSD-98-015-0805. The crystal structure is cubic with '*d'* spacing 2.43(6) Å. Here, crystallinity increases with increase in temperature.

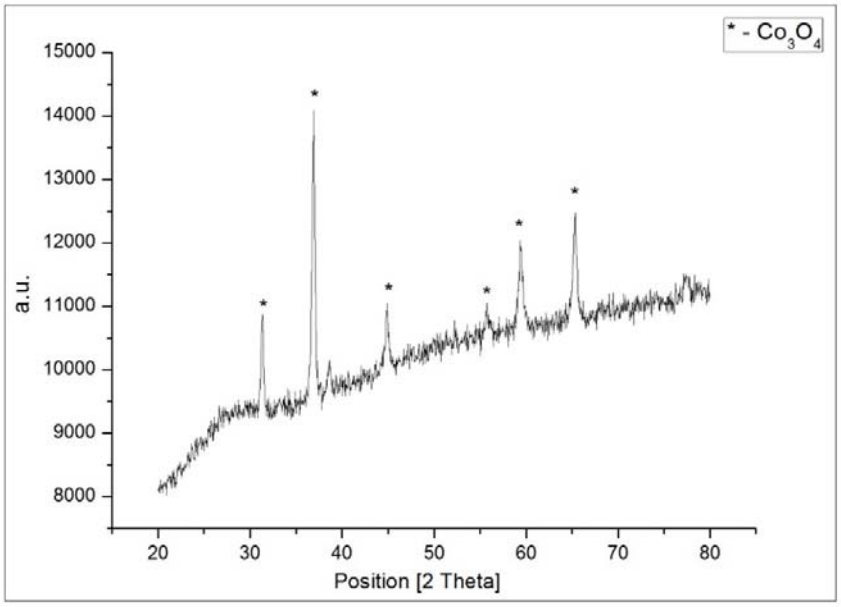


*Figure 9: XRD patterns of $Co(OH)_2$ calcined at $500^0C$.*

Figure 10, 11 and 12 show XRD patterns of as synthesized Co-Ni-$(OH)_2$, Co-Ni-$(OH)_2$ calcined at $300^0$C and $500^0$C respectively. The XRD patterns of as synthesized Co-Ni-$(OH)_2$ match with ICSD-98-002-6763. The compound found is $Co(OH)_2$.The crystal structure is cubic.

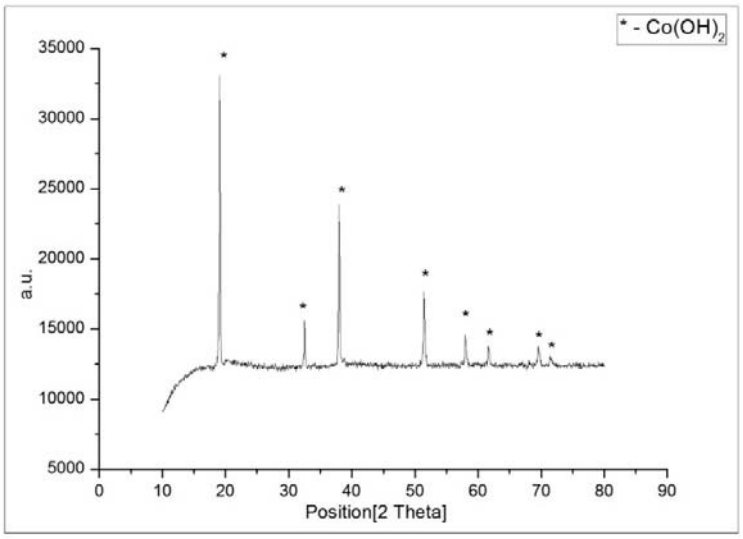


*Figure 10: XRD patterns of as synthesized Co-Ni-$(OH)_2$*

Figure 11 shows XRD patterns of Co-Ni-$(OH)_2$ calcined at $300^0$C. All the peaks correspond to Nickel Dicobalt (III) Oxide which matches with ICSD-98-002-4211. The crystal structure is cubic and '*d*' spacing is 2.44(6) Å.

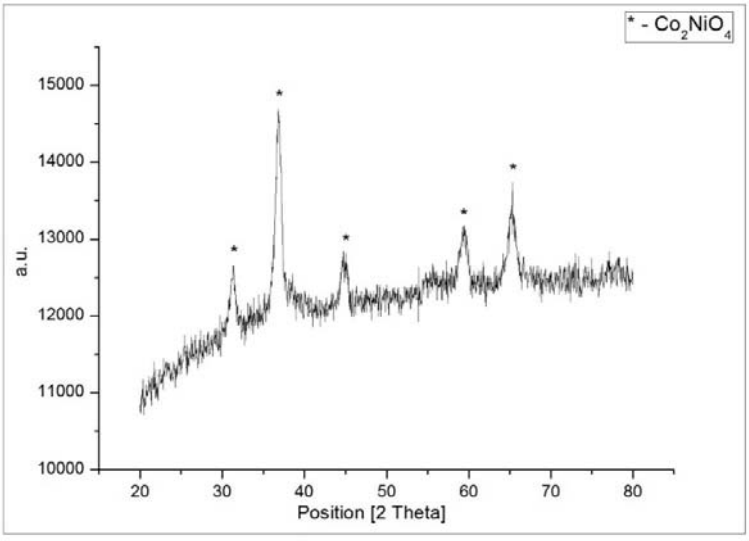


*Figure 11: XRD patterns of Co-Ni-$(OH)_2$ calcined at $300^0$C.*

Figure 12 shows XRD patterns of Co-Ni-$(OH)_2$ calcined at $500^0$C. All the peaks correspond to Nickel Dicobalt (III) Oxide which matches with ICSD-98-002-4211. The crystal structure is cubic and '*d*' spacing is 2.44(6) Å.

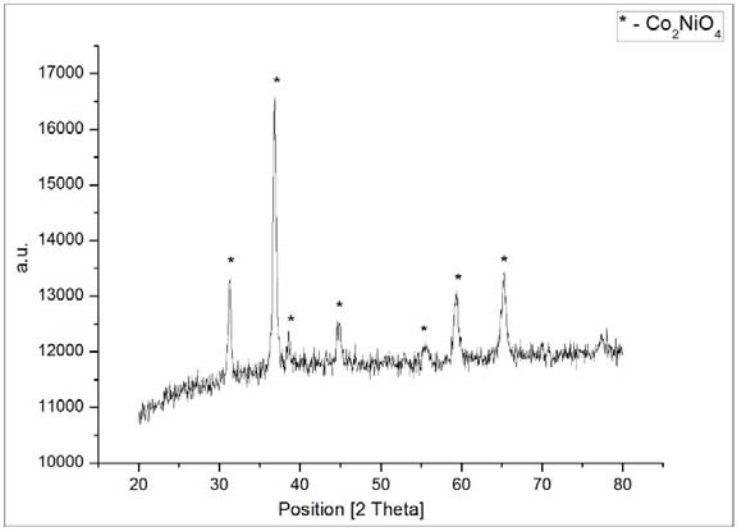


*Figure 12: XRD patterns of Co-Ni-$(OH)_2$ calcined at $500^0$C*

## 4.3 Field Emission Scanning Electron Microscopy:

FESEM images in figure 13, 14 and 15 show the microstructure of as synthesized nickel hydroxide powders and nickel hydroxide powders calcined at $300^0$C and $500^0$C, respectively. The images of as synthesized $Ni(OH)_2$ show spherical shaped structures. When calcined at $300^0$C the particles agglomerate to form some rod like structures. Upon increasing the calcination temperature to $500^0$C size of the spherical structures increases although the shape remains same.

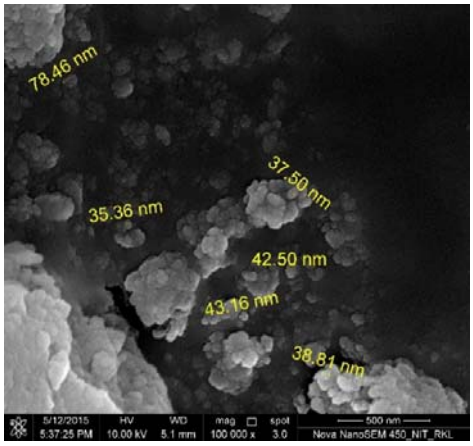


*Figure 13: FESEM image of as synthesized $Ni(OH)_2$*

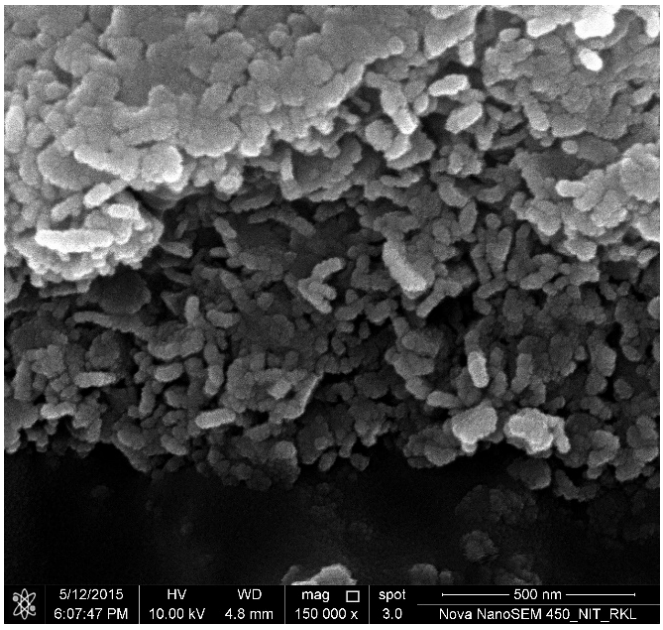


*Figure14: FESEM image of $Ni(OH)_2$ calcined at $300^0C$*

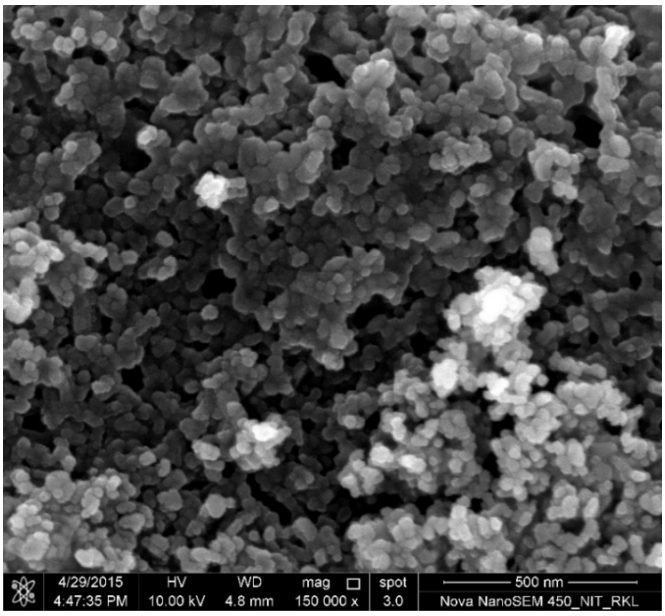


*Figure15: FESEM image of $Ni(OH)_2$ calcined at $500^0C$*

FESEM images in Figure 16, 17 and 18 show as synthesized cobalt hydroxide, cobalt hydroxide calcined at $300^0$C and $500^0$C, respectively. From the as synthesized image well defined polyhedral structures can be seen. When calcined at $300^0$C the particles tend to agglomerate. The edges becomes smoother upon calcining further at $500^0$ C.

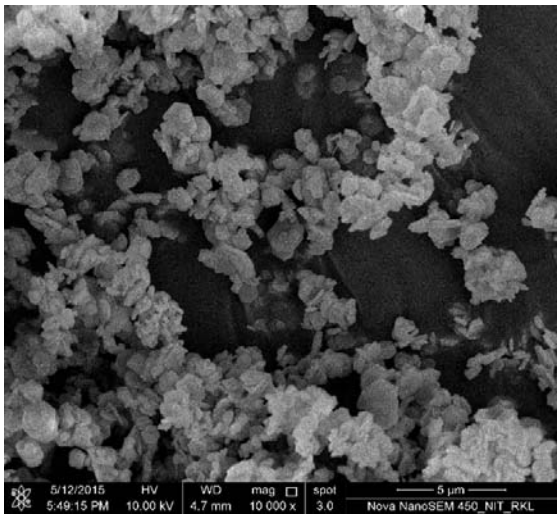


*Figure 146: FESEM image of as synthesized $Co(OH)_2$*

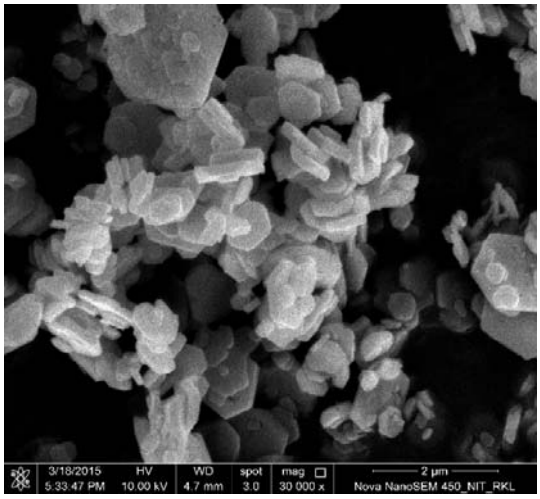


*Figure 157: FESEM image of $Co(OH)_2$ calcined at $300^0C$*

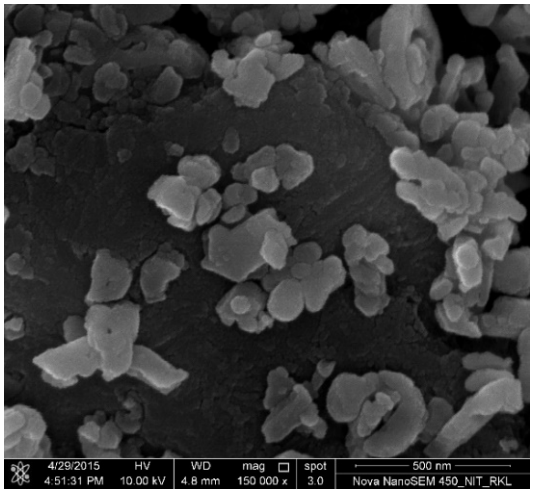


*Figure 168: FESEM image of $Co(OH)_2$ calcined at $500^0C$*

Figures 19, 20 and 21 show FESEM images of as synthesized Ni-doped cobalt hydroxide powder and the powders calcined at $300^0$C and $500^0$C, respectively. Well defined polyhedral structures can be observed. When calcined the as synthesized sample the shapes get disoriented and by increasing the temperature further small pores seem to appear on the surface of the sample.

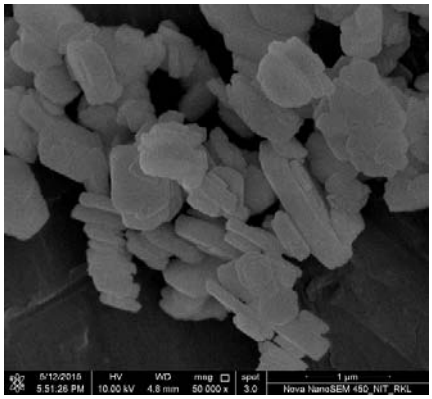

*Figure 179: FESEM image of as synthesized cobalt-nickel hydroxide*

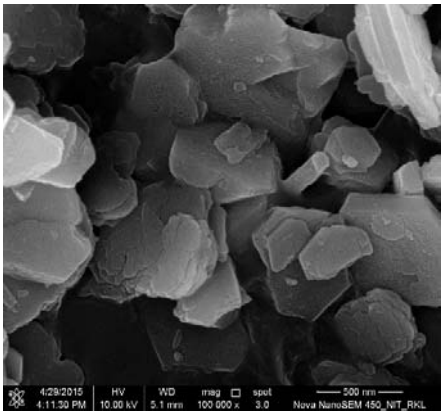

*Figure 20: FESEM image of cobalt-nickel hydroxide calcined at $300^0$C*

*Figure 21: FESEM image of cobalt-nickel hydroxide calcined at $500^0$C*

## 4.4 Microstructural Analysis:

Figure 22 to 28 show the EDS mapping image of as synthesized $Ni(OH)_2$, $Co(OH)_2$ and Co-Ni-$(OH)_2$. The images show homogenous distribution of the Ni/Co, O in the synthesized sample.

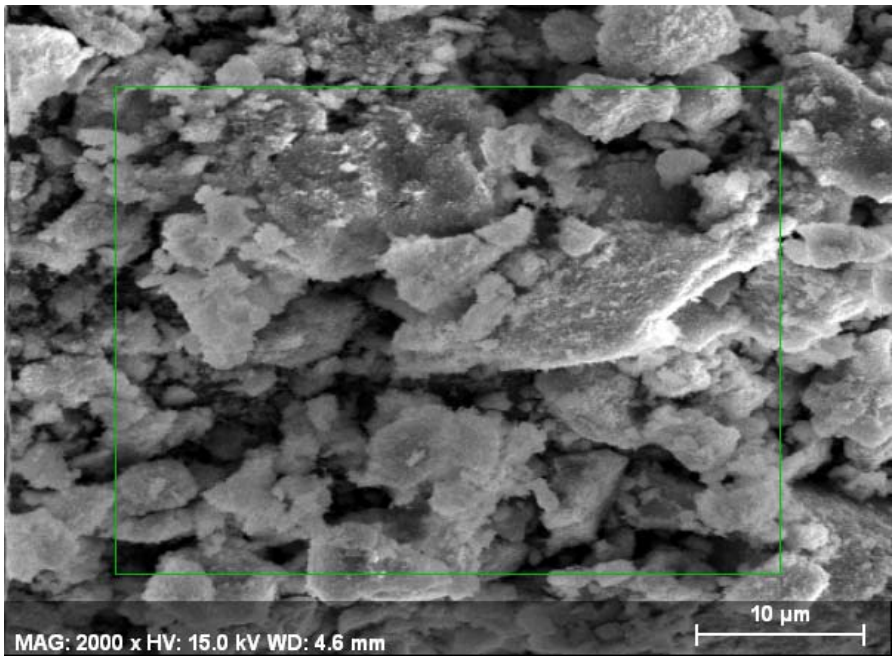


*Figure 22: Microstructure of $Ni(OH)_2$*

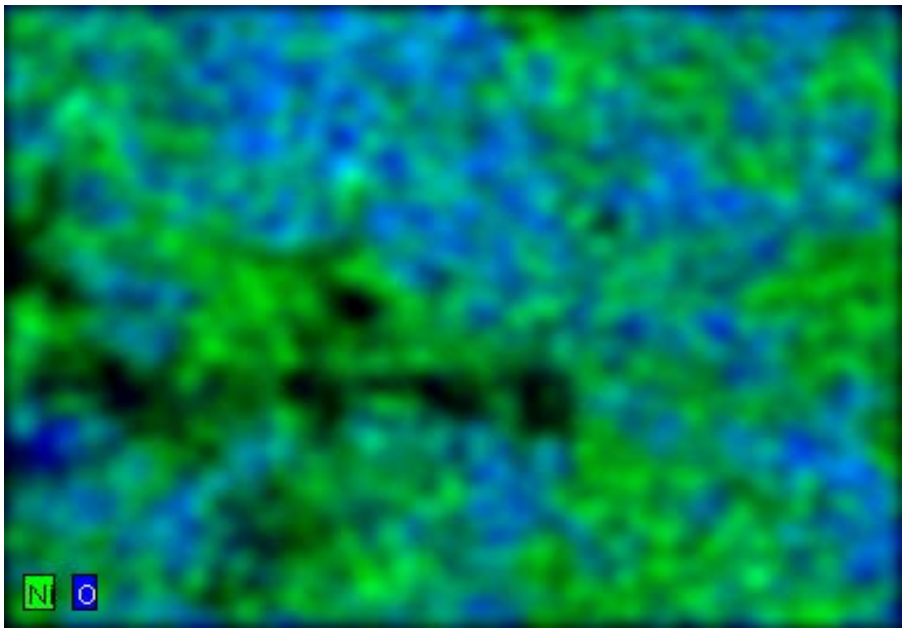


*Figure 23: EDS mapping image of $Ni(OH)_2$*

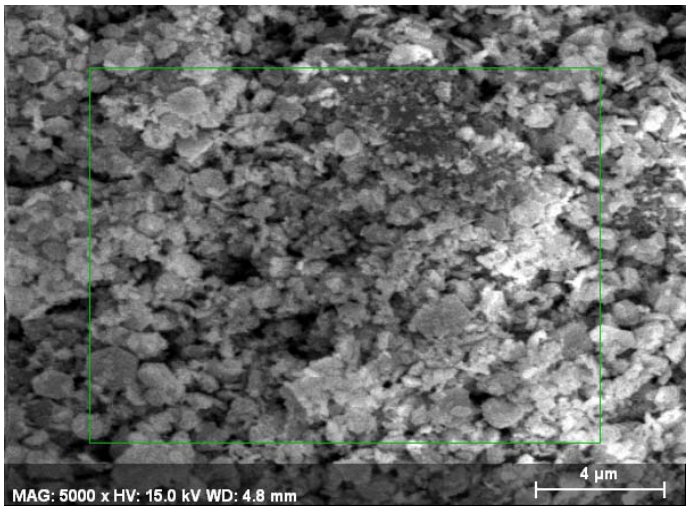


*Figure 24: Microstructure of $Co(OH)_2$*

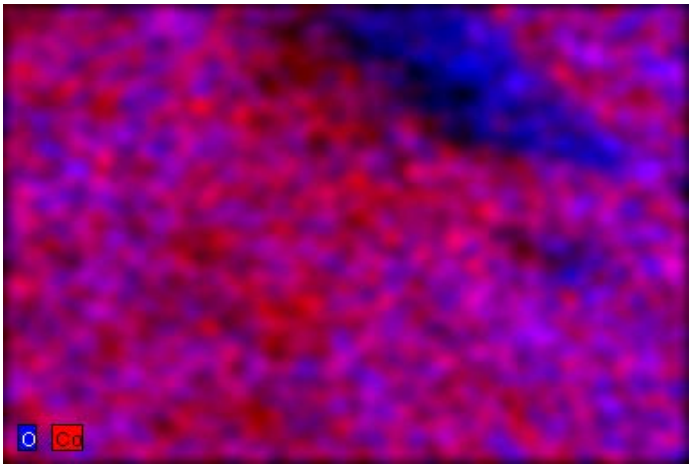


*Figure 25: EDS mapping image of $Co(OH)_2$*

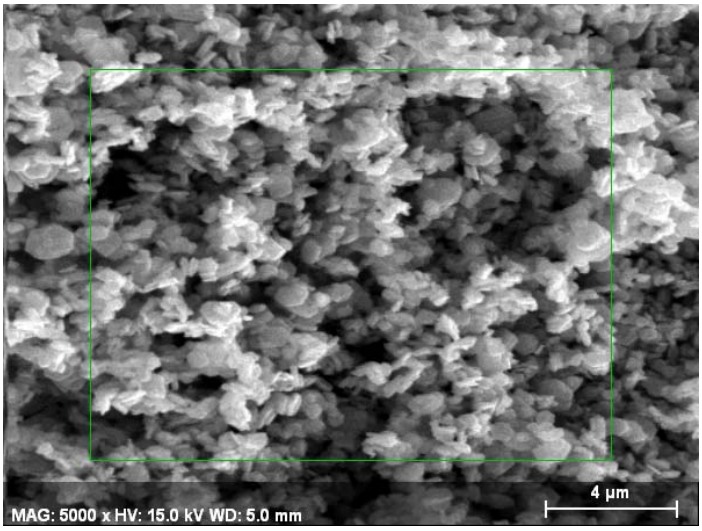


*Figure 26: Microstructure of Co-Ni-$(OH)_2$*

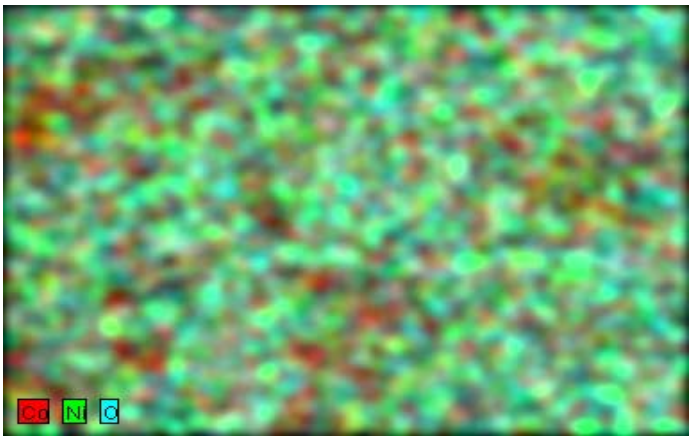


*Figure 27: EDS mapping image of Co-Ni-$(OH)_2$*

From Fig. 26 it can be found out that in the Ni-doped cobalt hydroxide prepared has the same ratio of cobalt and nickel that we have taken during the synthesis.

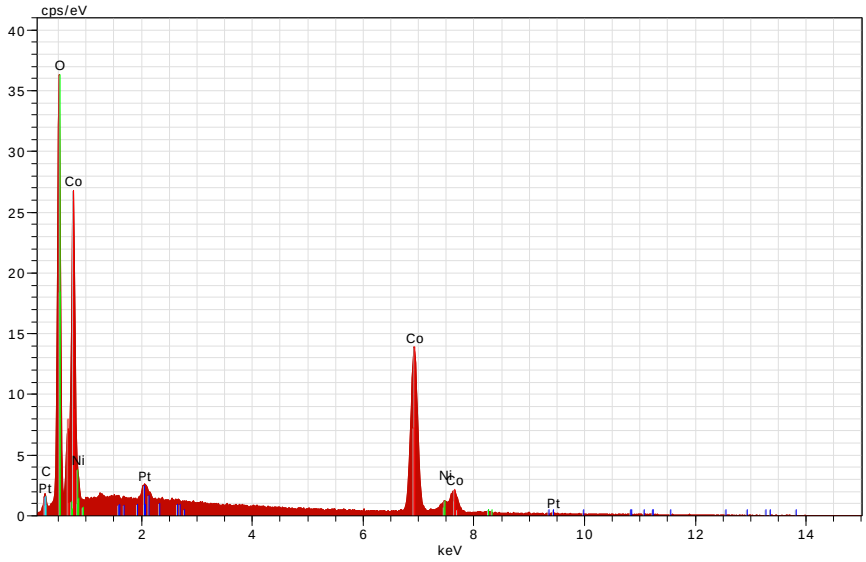


Spectrum: Sample 1 1925

| El | AN | Series | Net unn. C [wt.%] | norm. C [wt.%] | Atom. C [at.%] | Error (1 Sigma) [wt.%] |
|---|---|---|---|---|---|---|
| Co | 27 | K-series | 37983 | 60.61 | 66.99 | 38.20 | 1.86 |
| O | 8 | K-series | 36053 | 23.43 | 25.89 | 54.38 | 2.86 |
| Ni | 28 | K-series | 2695 | 5.07 | 5.60 | 3.21 | 0.22 |
| C | 6 | K-series | 707 | 1.36 | 1.51 | 4.22 | 0.37 |
| Pt | 78 | M-series | 2366 | 0.00 | 0.00 | 0.00 | 0.00 |
| | | Total: | | 90.48 | 100.00 | 100.00 | |

*Figure 28: EDS spectrum of Co-Ni-$(OH)_2$*

## 4.5 Photoluminescence:

To check the photoluminescence properties, the samples were excited at a wavelength of 450 nm. The graphs in figure 29 to 31 are the excitation graphs of the as synthesized samples.

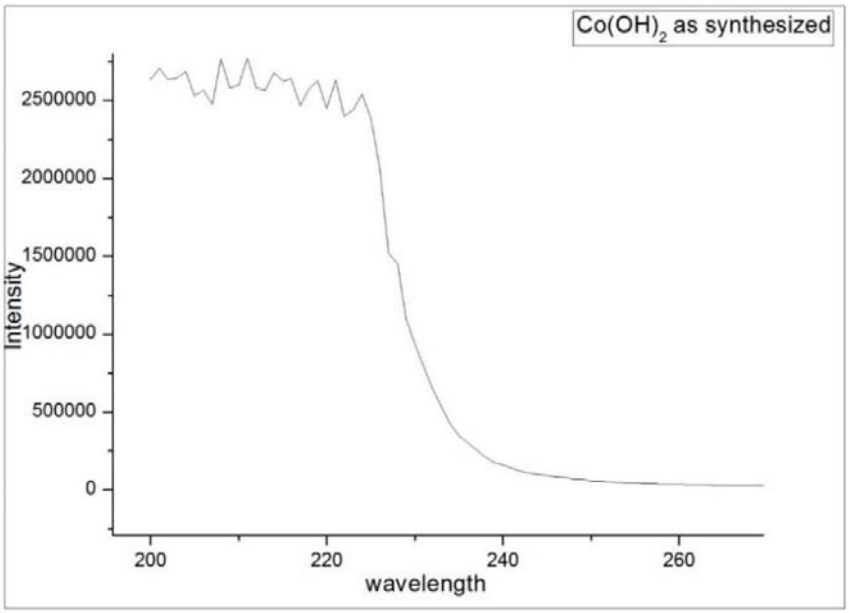


*Figure 29: Excitation spectrum of as synthesized $Co(OH)_2$*

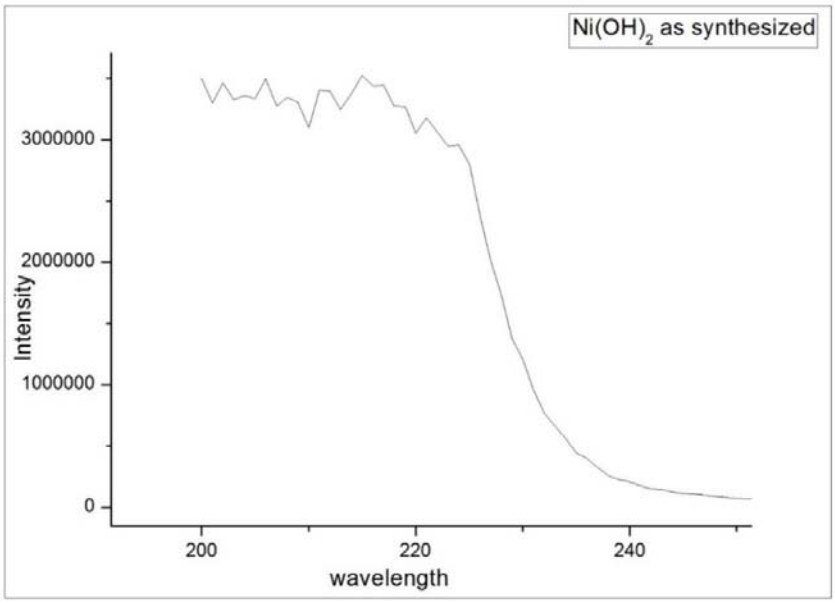


*Figure 30: Excitation spectrum of as synthesized $Ni(OH)_2$*

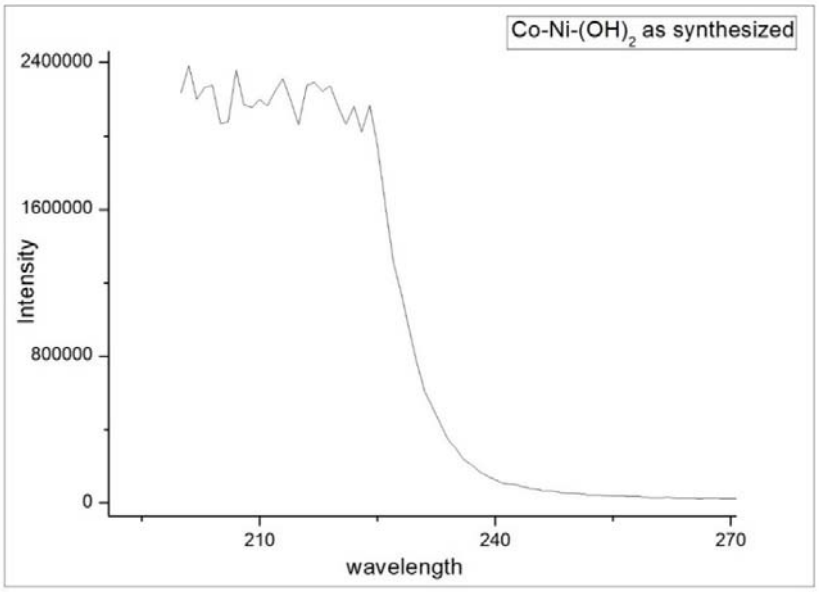


*Figure 31: Excitation spectrum of as synthesized Co-Ni-$(OH)_2$*

The above excitation spectrum graphs show a peak around wavelength of 220nm. Based on the excitation sepctra, the emission spectra of all samples were analysed with an excitation wavelength of 220 nm.

The intensity vs wavelength graphs of as synthesized $Ni(OH)_2$, $Co(OH)_2$, Co-Ni-$(OH)_2$ are presented in Figure 32 to 34.

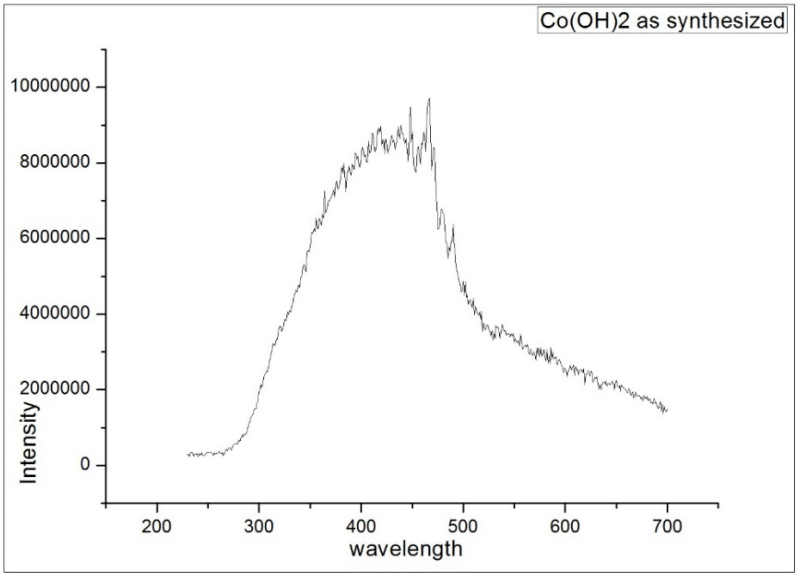


*Figure 32: Emission spectrum of as synthesized Co-$(OH)_2$*

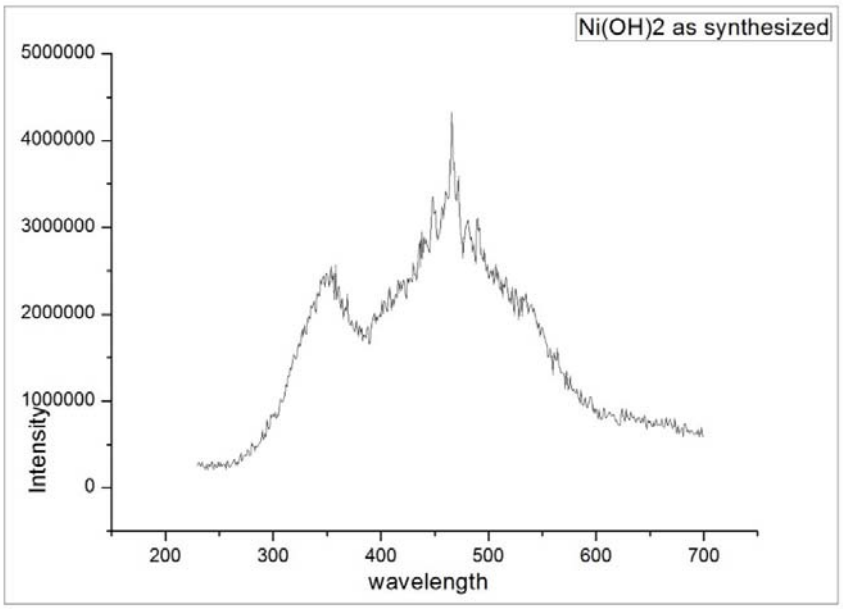


*Figure 33: Emission spectrum of as synthesized Co-Ni-$(OH)_2$*

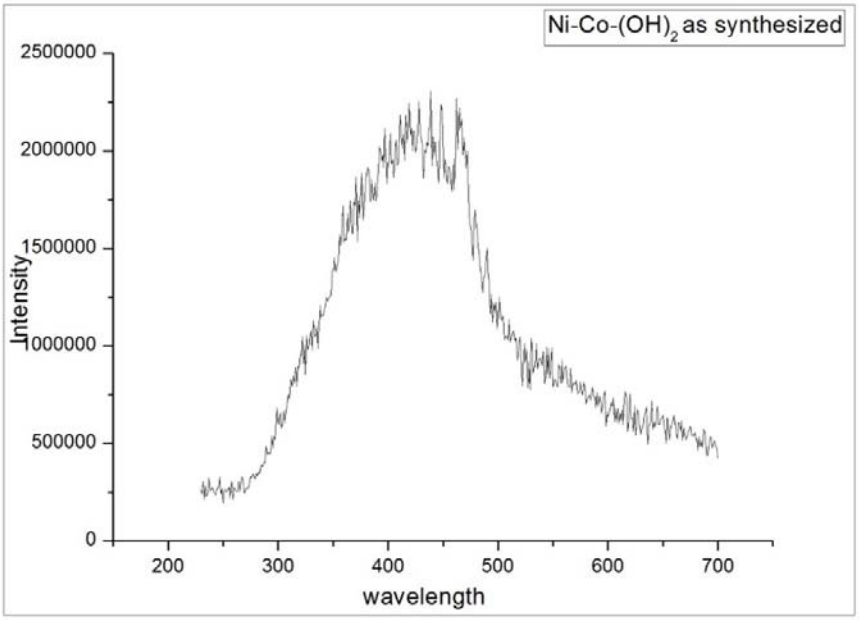


-

*Figure 34: Emission spectrum of Co-Ni-$(OH)_2$*

In the emission spectrum of $Co(OH)_2$ a broad peak was observed ranging from 275nm to 700nm centred at around 430nm which is in the violet-blue region. In case of $Ni(OH)_2$ a

broad peak ranging from 275nm to 700nm was observed which is centred at two points i.e. at 350nm and at 460nm. The second peak falls in near blue region. In case of the doped sample the centre of the peak again shift towards the violet blue region.

Figure 35 to 37 show the intensity vs wavelength graph of the calcined samples at $300^0$C. In the first graph it can be observed that $Co(OH)_2$ does not show any peak at visible region. But $Ni(OH)_2$ instead shows a broad peak ranging from 250nm to 700nm centred at around 430 nm but with much less intensity than the as synthesized sample. But, it falls in the violet-blue region. The doped sample also shows a broad peak ranging from 275nm to 700 nm centred at 420 nm which also falls in the violet blue region. But the intensity is further less than the $Ni(OH)_2$ sample. The doped sample illustrates photoluminescence properties due to the $Ni(OH)_2$ present and intensity is low because the ratio in which it is taken with $Co(OH)_2$ is very less.

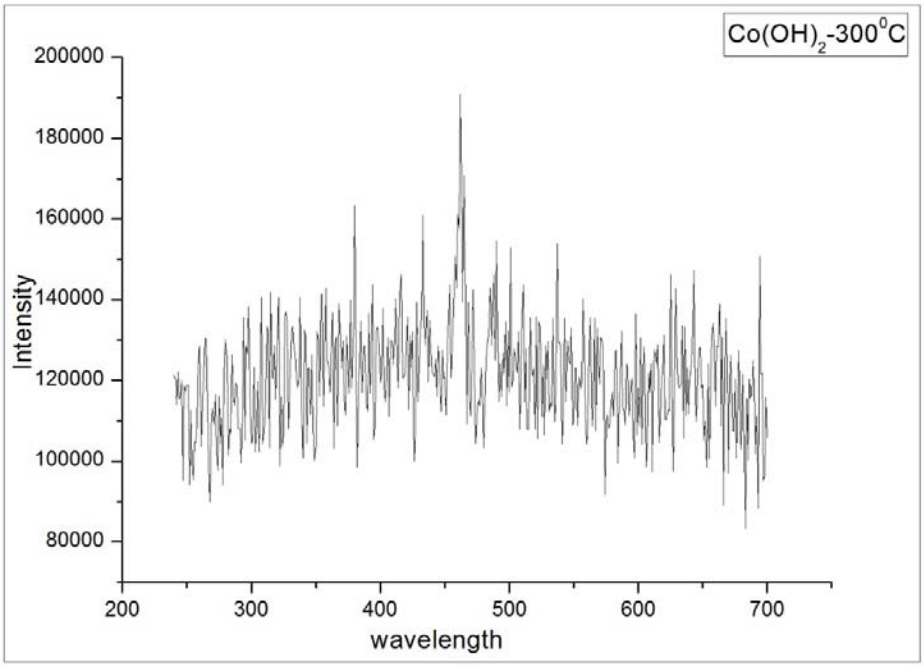


*Figure 35: Emission spectrum of $Co(OH)_2$ calcined at $300^0$C*

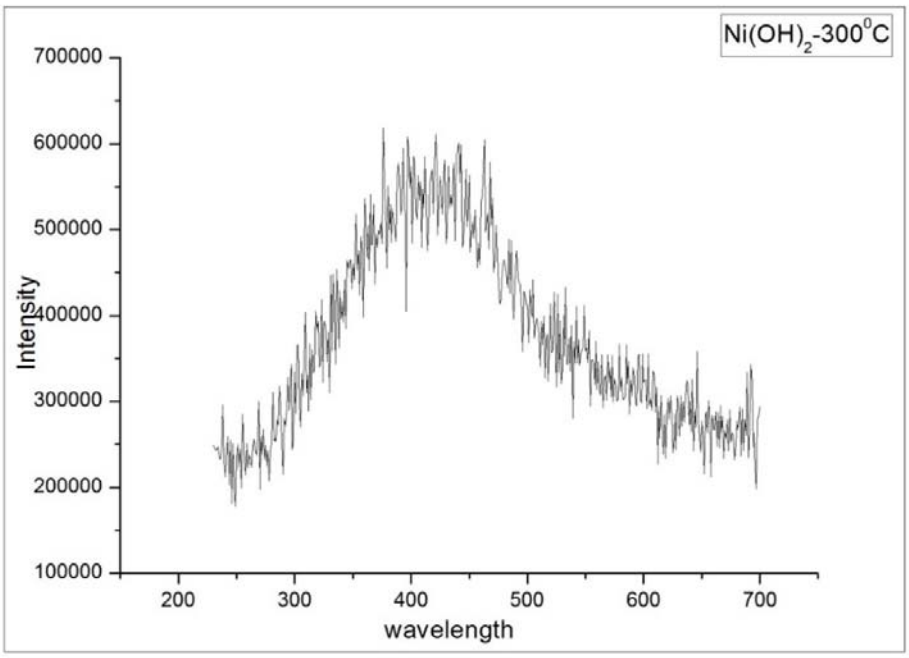


*Figure 36: Emission spectrum of $Ni(OH)_2$ calcined at $300^0C$*

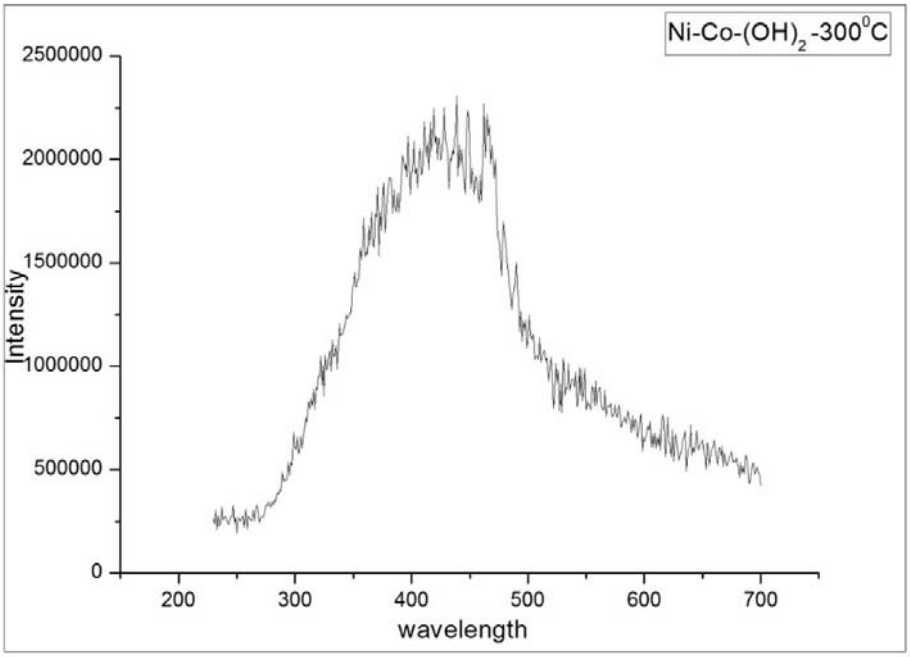


*Figure 37: Emission spectrum of Co-Ni-$(OH)_2$ calcined at $300^0C$*

## CONCLUSIONS:

Hydroxides of nickel, cobalt and a Ni-doped cobalt has been prepared through precipitation route. After obtaining hydroxide powders they were calcined at $300^0$C and $500^0$C. Then various characterization were done like DSC-TG, FESEM, XRD analysis. From the stated characterizations a polyhedral structured cobalt hydroxide and a nearly spherical structured nickel hydroxide was found. The characteristics of the doped samples were comparable to the cobalt hydroxide as the ratio of cobalt hydroxide and nickel hydroxide in it was 9:1. The calcined hydroxides have transformed into oxides which showed a slightly altered properties than the hydroxide. Photoluminescence properties of the hydroxides and oxides were tested. All the hydroxides showed good photoluminescence properties. But only the oxide of nickel was found to be photoluminescent. The cobalt oxide did not show any kind of photoluminescence, while doped sample having little amount of nickel showed a weaker luminescence property with a lower intensity than the hydroxides.

## REFERENCE:


1. D.P. Dubal, V.J. Fulari, C.D. Lokhande, Microporous and Mesoporous Materials 151 (2012) 511–516
2. Changyu Li and Shouxin Liu, Journal of Nanomaterials Volume 2012, Article ID 648012
3. Venkataramana Bonu, Arindam Das, S. Amirthapandian, Sandip Dharaa and Ashok Kumar Tyagia, Phys.Chem.Chem.Phys., 2015, 17, 9794
4. F. Cao*, G.X. Pan, P.S. Tang, H.F. Chen, Journal of Power Sources 216 (2012) 395e399
5. Yumei Ren, Li Wang, Zhongjia Dai, Xiankun Huang, Jianjun Li, Ning Chen, Jian Gao, Hailei Zhao, Xiaoming Sun, Xiangming He, Int. J. Electrochem. Sci., 7 **(2012)** 12236 – 12243
6. Quansheng Songa,b,*, Zhiyuan Tanga, Hetong Guoa, S.L.I. Chan, Journal of Power Sources 112 (2002) 428–434
7. Wei Xing, Feng Li, Zi-feng Yan, G.Q. Lua, Journal of Power Sources 134 (2004) 324–330
8. ZHANG YongQi, XIA XinHui, KANG Jing & TU JiangPing, Chinese Science Bulletin, November 2012 Vol.57 No.32: 4215-4219
9. DongEn Zhang, LiZheng Ren, XiaoYun Hao, BingBing Pan, MingYan Wang, JuanJuan Ma, Feng Li, ShuAn Li, ZhiWei Tonga, Applied surface science- 30111
10. Guoping Wang, Lei Zhang, Jenny Kim, Jiujun Zhang, Journal of Power Sources 217 (2012) 554e561
11. Jinxiu Li, Mei Yang, Jinping Wei and Zhen Zhou, Nanoscale, 2012, 4, 449
12. Wenzhong Wang n, Jie Xu, Physica E 69(2015) 19-23
13. Yajun Qi, Hongyan Qi, Chaojing Lu, Ye Yang, Yong Zhao, J Mater Sci: Mater Electron (2009) 20:479–483